



# Elucidation of reaction mechanisms of Ni<sub>2</sub>SnP in Li-ion and Na-ion systems



C. Marino <sup>a,\*</sup>, N. Dupré <sup>b</sup>, C. Villevieille <sup>a,\*\*</sup>

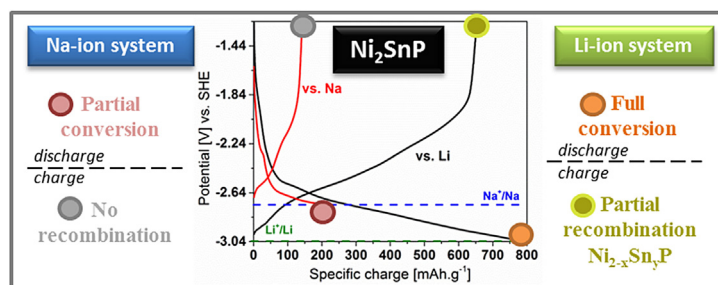
<sup>a</sup> Paul Scherrer Institut, Electrochemistry Laboratory, Villigen PSI, Switzerland

<sup>b</sup> Institut des Matériaux Jean Rouxel (IMN), CNRS UMR 6502, Université de Nantes, Nantes, France

## HIGHLIGHTS

- Electrochemical performance of Ni<sub>2</sub>SnP for Li-ion and Na-ion batteries.
- Specific charge close to the theoretical one (742 mAh.g<sup>-1</sup>) reached in the Li system.
- Only 200 mAh.g<sup>-1</sup> are obtained in the Na system.
- Different electrochemical mechanisms in Li-ion and Na-ion batteries.

## GRAPHICAL ABSTRACT



## ARTICLE INFO

### Article history:

Received 5 July 2017

Received in revised form

15 August 2017

Accepted 26 August 2017

### Keywords:

Negative electrode

Na-ion battery

Li-ion battery

Conversion material

X-ray absorption spectroscopy

NMR spectroscopy

## ABSTRACT

Electrochemical performance of Ni<sub>2</sub>SnP was assessed in Li-ion and Na-ion battery systems. When cycled versus Li, Ni<sub>2</sub>SnP exhibited a reversible specific charge of 700 mAh.g<sup>-1</sup> (theoretical specific charge: 742 mAh.g<sup>-1</sup>). In the Na system, the specific observed charge was ca. 200 mAh.g<sup>-1</sup> (theoretical specific charge: 676 mAh.g<sup>-1</sup>). X-ray diffraction, Ni K-edge X-ray absorption spectroscopy, and <sup>31</sup>P and <sup>7</sup>Li/<sup>23</sup>Na nuclear magnetic resonance spectroscopy were used to elucidate the electrochemical mechanisms in both systems. Versus Li, Ni<sub>2</sub>SnP undergoes a conversion reaction resulting in the extrusion of Ni and the alloying of Li-Sn and Li-P. On delithiation, the material partially recombines into a Sn- and Ni-deficient form. In the Na system, Ni<sub>2</sub>SnP reacts through the conversion of P into Na<sub>3</sub>P. These results indicate that the recombination of the pristine material (even partially) increases cycling stability.

© 2017 Elsevier B.V. All rights reserved.

## 1. Introduction

In recent years, the market for portable electronic devices has increased exponentially. Hence, improvements in battery technologies are crucial to increase the practicality, performance, and portability of these devices. The performance of Li- or Na-based batteries may be increased by incorporating novel electrode materials with high energy densities; for instance, by replacing graphite, which is commonly used as the negative electrode

\* Corresponding author. Paul Scherrer Institute, CH-5232 Villigen PSI, Switzerland.

\*\* Corresponding author. Paul Scherrer Institute, CH-5232 Villigen PSI, Switzerland.

E-mail addresses: [Cyril.marino@psi.ch](mailto:Cyril.marino@psi.ch) (C. Marino), [Claire.villevieille@psi.ch](mailto:Claire.villevieille@psi.ch) (C. Villevieille).

(theoretical specific charge:  $372 \text{ mAh.g}^{-1}$ ), by alloying/conversion materials with theoretical specific charge higher than  $500 \text{ mAh.g}^{-1}$  [1,2].

Despite their large volume change upon cycling, conversion/alloying-based materials are considered as suitable alternatives to graphite [3,4]. Binary and ternary materials have been reported, in which one or two active elements are combined with a single inactive element. The purpose of the inactive material is to create a local conductive matrix that facilitates the alloying/conversion reaction of the active elements and to buffer the volume changes that occur during cycling. The electrochemical properties of composite materials such as Co-Sn-Sb [5], Ni-Co-Sn [6], and Ni-Sn-P [7] have been reported. In particular, TiSnSb [8] exhibited very promising electrochemical performance. The reaction mechanisms of these materials involve the total or partial recombination of the ternary phase after the first cycle. As a result, they exhibit good cycling stability after more than 50 cycles.

Recently, we investigated various Sn-based materials [9,10]. We found that Mn-Sn-based materials exhibited excellent reversibility in Na-ion batteries, as a result of the development of a ternary phase during cycling and the recombination of the pristine Mn-Sn phase after a single cycle. Co-Sn exhibited the opposite trend and poor electrochemical properties because of the rapid extrusion of Co. We also reported an Sb-based ternary phase,  $\text{CuSbS}_2$ , as an electrode material for Na-ion batteries [11]. This material exhibited a specific charge of  $730 \text{ mAh.g}^{-1}$  in a Na-ion battery and  $450 \text{ mAh.g}^{-1}$  in a Li-ion battery [12]. Xia et al. reported a reversible specific charge of  $500 \text{ mAh.g}^{-1}$  for  $\text{Ni}_2\text{SnP}$  in a Li-ion system; however, the electrochemical reaction mechanism was not elucidated [13]. The advantage of  $\text{Ni}_2\text{SnP}$  compared to binary  $\text{SnP}_x$  compounds results in the presence of the inactive and conductive Ni matrix, which could reduce the lack of electronic conductivity once the volume changes occur through the reaction with Li/Na. In the present study, we elucidated the reaction mechanisms of  $\text{Ni}_2\text{SnP}$  in Li-ion and Na-ion systems by analysing these systems using X-ray diffraction (XRD), Ni K-edge X-ray absorption spectroscopy (XAS), and  $^{31}\text{P}$ ,  $^7\text{Li}$ , and  $^{23}\text{Na}$  nuclear magnetic resonance spectroscopy (NMR).

## 2. Experimental section

### 2.1. Synthesis

$\text{Ni}_2\text{SnP}$  was synthesised via mechano-synthesis by combining a stoichiometric amount of nickel (99.8%, 325-mesh; Alfa Aesar), tin (99.8%, 325 mesh; Alfa Aesar) with red phosphorus (99.99%, Sigma-Aldrich) in a 45-mL stainless steel ball mill (Pulverisette 7, Fritsch) containing 30 balls (diameter: 5 mm) under Ar. The reaction was conducted at 800 rpm for a total of 33 h (99 cycles: 10 min active/10 min inactive).

### 2.2. Electrochemistry

Electrode slurries were prepared using a ball milling technique to ensure the thorough dispersal of active material/binder/carbon. Typically, a mixture of 70%<sub>wt</sub>  $\text{Ni}_2\text{SnP}$ , 9%<sub>wt</sub> carbon black (CB; SuperC65, Imerys), 9%<sub>wt</sub> vapour-grown carbon fibres (VGCF; Showa Denko) and 12%<sub>wt</sub> carboxymethylcellulose sodium salt (CMC; Alfa Aesar) was ball milled in deionised water. The obtained slurry was cast onto copper foil (used as a current collector) and dried under air at room temperature. Electrodes (diameter: 13 mm) with an active material loading of around  $5.5 \text{ mg cm}^{-2}$  were punched and dried under dynamic vacuum at  $120^\circ\text{C}$  for 2 h. Electrochemical cells were assembled in an Ar-filled glove box using a glass fibre separator and either metallic sodium or metallic lithium as the

counter electrode. In the Li-ion system, 1 M  $\text{LiPF}_6$  dissolved in ethylene carbonate:dimethyl carbonate (EC:DMC, LP30) was used as the electrolyte. In the Na-ion system, 1 M  $\text{NaClO}_4$  dissolved in propylene carbonate (PC) was used as the electrolyte. The cell performances were measured at  $25^\circ\text{C}$  using an Astrol cycling device in galvanostatic mode between 5 mV and 1.8 V (versus  $\text{Li}^+/\text{Li}$  or  $\text{Na}^+/\text{Na}$ ) at a C/40 rate (40 h for a full charge or discharge considering a theoretical specific charge of  $742 \text{ mAh.g}^{-1}$ ).

### 2.3. X-ray diffraction (XRD)

XRD measurements were performed in reflection mode at  $25^\circ\text{C}$  with a PANalytical Empyrean diffractometer using  $\text{Cu K}\alpha$ -radiation. Capillary mode (0.3 mm diameter capillaries) was used to measure ex situ samples prepared from pristine and cycled electrodes. The patterns presented herein are the sum of 12 patterns acquired over 1 h from  $15^\circ$  to  $70^\circ$  with a step size of  $0.0334^\circ$ . Operando measurements were performed using a homemade in situ cell [14] with a powder electrode consisting of 70%<sub>wt</sub> active material, 20%<sub>wt</sub> CB, and 10%<sub>wt</sub> VGCF. Currents similar to those described in the above section were applied. Each pattern was acquired for 1 h from  $20^\circ$  to  $55^\circ$  with a step size of  $0.0334^\circ$ .

### 2.4. Scanning electron microscopy (SEM)

SEM measurements were performed using a Carl Zeiss Ultra55 scanning electron microscope in secondary electron mode at 3 kV.

### 2.5. X-ray absorption spectroscopy (XAS)

The electrodes were cycled galvanostatically until reaching the desired potential. Subsequently, a long potentiostatic step was used to ensure that the electrochemical reaction proceeded thoroughly. After disassembling the cell, the electrode material was removed from the current collector and the resulting powder was washed with dimethylcarbonate (DMC). The powder was then mixed with CB to dilute the electrode material and fill a 1 mm diameter capillary. XAS measurements were performed in transmission mode using the SuperXAS beamline at the Swiss Light Source (SLS; PSI, Switzerland) at the Ni K-edge (8347 eV) using a quick EXAFS monochromator [15] with an acquisition time of 50 ms. The spectra presented herein were produced from the summation of 2400 spectra (total acquisition time: 2 min). The spectra were calibrated using a reference Ni foil, placed after the sample. Data were analysed using Athena and Artemis softwares [16].

### 2.6. Nuclear magnetic resonance spectroscopy (NMR)

NMR samples were prepared as for the electrochemical experiments (above), except that powder electrodes of 35 mg active material were used instead of standard ones. The powder electrodes were cycled using 1 M  $\text{LiClO}_4$  in EC:DMC as the electrolyte. Lithium perchlorate was used instead of lithium hexafluorophosphate to prevent overlapping of the phosphorus signal originating from the electrode with one originating from the electrolyte. After cycling, the powder electrodes were washed with DMC and placed in a 2.5 mm diameter zirconia rotor. MAS-NMR measurements were acquired using a Bruker Avance 500 spectrometer ( $B = 11.8 \text{ T}$ ) using Larmor frequencies of 194.37, 132.29, and 202.45 MHz, for  $^7\text{Li}$ ,  $^{23}\text{Na}$ , and  $^{31}\text{P}$ , respectively. Single-pulse  $^7\text{Li}$  NMR was performed at a spin rate of 25 kHz with a pulse length of 1.4  $\mu\text{s}$  and a recycle time of 5 s.  $^{23}\text{Na}$  NMR spectra were acquired at a spin rate of 25 kHz; an echo sequence was used to remove the distorted baseline (90° pulse length: 1.0  $\mu\text{s}$ ; recycle time: 5 s). Single-pulse  $^{31}\text{P}$  NMR was performed at a spin rate of 25 kHz with a

Download English Version:

<https://daneshyari.com/en/article/5148752>

Download Persian Version:

<https://daneshyari.com/article/5148752>

[Daneshyari.com](https://daneshyari.com)